

Search for a heavy Majorana neutrino in lepton number violating decays of $D \rightarrow K\pi e^+e^+$

M. Ablikim¹, M. N. Achasov^{10,d}, S. Ahmed¹⁵, M. Albrecht⁴, M. Alekseev^{56A,56C}, A. Amoroso^{56A,56C}, F. F. An¹, Q. An^{53,43}, J. Z. Bai¹, Y. Bai⁴², O. Bakina²⁷, R. Baldini Ferroli^{23A}, Y. Ban³⁵, K. Begzsuren²⁵, D. W. Bennett²², J. V. Bennett⁵, N. Berger²⁶, M. Bertani^{23A}, D. Bettoni^{24A}, F. Bianchi^{56A,56C}, E. Boger^{27,b}, I. Boyko²⁷, R. A. Briere⁵, H. Cai⁵⁸, X. Cai^{1,43}, O. Cakir^{46A}, A. Calcaterra^{23A}, G. F. Cao^{1,47}, S. A. Cetin^{46B}, J. Chai^{56C}, J. F. Chang^{1,43}, G. Chelkov^{27,b,c}, G. Chen¹, H. S. Chen^{1,47}, J. C. Chen¹, M. L. Chen^{1,43}, P. L. Chen⁵⁴, S. J. Chen³³, X. R. Chen³⁰, Y. B. Chen^{1,43}, W. Cheng^{56C}, X. K. Chu³⁵, G. Cibinetto^{24A}, F. Cossio^{56C}, H. L. Dai^{1,43}, J. P. Dai^{38,h}, A. Dbeysi¹⁵, D. Dedovich²⁷, Z. Y. Deng¹, A. Denig²⁶, I. Denysenko²⁷, M. Destefanis^{56A,56C}, F. De Mori^{56A,56C}, Y. Ding³¹, C. Dong³⁴, J. Dong^{1,43}, L. Y. Dong^{1,47}, M. Y. Dong^{1,43,47}, Z. L. Dou³³, S. X. Du⁶¹, P. F. Duan¹, J. Fang^{1,43}, S. S. Fang^{1,47}, Y. Fang¹, R. Farinelli^{24A,24B}, L. Fava^{56B,56C}, S. Fegan²⁶, F. Feldbauer⁴, G. Felici^{23A}, C. Q. Feng^{53,43}, E. Fioravanti^{24A}, M. Fritsch⁴, C. D. Fu¹, Q. Gao¹, X. L. Gao^{53,43}, Y. Gao⁴⁵, Y. G. Gao⁶, Z. Gao^{53,43}, B. Garillon²⁶, I. Garzia^{24A}, A. Gilman⁵⁰, K. Goetzen¹¹, L. Gong³⁴, W. X. Gong^{1,43}, W. Gradl²⁶, M. Greco^{56A,56C}, M. H. Gu^{1,43}, Y. T. Gu¹³, A. Q. Guo¹, R. P. Guo^{1,47}, Y. P. Guo²⁶, A. Guskov²⁷, Z. Haddadi²⁹, S. Han⁵⁸, X. Q. Hao¹⁶, F. A. Harris⁴⁸, K. L. He^{1,47}, X. Q. He⁵², F. H. Heinsius⁴, T. Held⁴, Y. K. Heng^{1,43,47}, Z. L. Hou¹, H. M. Hu^{1,47}, J. F. Hu^{38,h}, T. Hu^{1,43,47}, Y. Hu¹, G. S. Huang^{53,43}, J. S. Huang¹⁶, X. T. Huang³⁷, X. Z. Huang³³, Z. L. Huang³¹, T. Hussain⁵⁵, W. Ikegami Andersson⁵⁷, M. Irshad^{53,43}, Q. Ji¹, Q. P. Ji¹⁶, X. B. Ji^{1,47}, X. L. Ji^{1,43}, X. S. Jiang^{1,43,47}, X. Y. Jiang³⁴, J. B. Jiao³⁷, Z. Jiao¹⁸, D. P. Jin^{1,43,47}, S. Jin^{1,47}, Y. Jin⁴⁹, T. Johansson⁵⁷, A. Julin⁵⁰, N. Kalantar-Nayestanaki²⁹, X. S. Kang³⁴, M. Kavatsyuk²⁹, B. C. Ke¹, I. K. Keshk⁴, T. Khan^{53,43}, A. Khoukaz⁵¹, P. Kiese²⁶, R. Kiuchi¹, R. Kliemt¹¹, L. Koch²⁸, O. B. Kolcu^{46B,f}, B. Kopf⁴, M. Kornicer⁴⁸, M. Kuemmel⁴, M. Kuessner⁴, A. Kupsc⁵⁷, M. Kurth¹, W. Kühn²⁸, J. S. Lange²⁸, P. Larin¹⁵, L. Lavezzi^{56C}, H. Leithoff²⁶, C. Li⁵⁷, Cheng Li^{53,43}, D. M. Li⁶¹, F. Li^{1,43}, F. Y. Li³⁵, G. Li¹, H. B. Li^{1,47}, H. J. Li^{9,j}, J. C. Li¹, J. W. Li⁴¹, Jin Li³⁶, K. J. Li⁴⁴, Kang Li¹⁴, Ke Li¹, Lei Li³, P. L. Li^{53,43}, P. R. Li^{47,7}, Q. Y. Li³⁷, W. D. Li^{1,47}, W. G. Li¹, X. L. Li³⁷, X. N. Li^{1,43}, X. Q. Li³⁴, Z. B. Li⁴⁴, H. Liang^{53,43}, Y. F. Liang⁴⁰, Y. T. Liang²⁸, G. R. Liao¹², L. Z. Liao^{1,47}, J. Libby²¹, C. X. Lin⁴⁴, D. X. Lin¹⁵, B. Liu^{38,h}, B. J. Liu¹, C. X. Liu¹, D. Liu^{53,43}, D. Y. Liu^{38,h}, F. H. Liu³⁹, Fang Liu¹, Feng Liu⁶, H. B. Liu¹³, H. L. Liu⁴², H. M. Liu^{1,47}, Huanhuan Liu¹, Huihui Liu¹⁷, J. B. Liu^{53,43}, J. Y. Liu^{1,47}, K. Liu⁴⁵, K. Y. Liu³¹, Ke Liu⁶, L. D. Liu³⁵, Q. Liu⁴⁷, S. B. Liu^{53,43}, X. Liu³⁰, Y. B. Liu³⁴, Z. A. Liu^{1,43,47}, Zhigang Liu²⁶, Y. F. Long³⁵, X. C. Lou^{1,43,47}, H. J. Lu¹⁸, J. G. Lu^{1,43}, Y. Lu¹, Y. P. Lu^{1,43}, C. L. Luo³², M. X. Luo⁶⁰, T. Luo^{9,j}, X. L. Luo^{1,43}, S. Lusso^{56C}, X. R. Lyu⁴⁷, F. C. Ma³¹, H. L. Ma¹, L. L. Ma³⁷, M. M. Ma^{1,47}, Q. M. Ma¹, T. Ma¹, X. N. Ma³⁴, X. Y. Ma^{1,43}, Y. M. Ma³⁷, F. E. Maas¹⁵, M. Maggiora^{56A,56C}, S. Maldaner²⁶, Q. A. Malik⁵⁵, A. Mangoni^{23B}, Y. J. Mao³⁵, Z. P. Mao¹, S. Marcello^{56A,56C}, Z. X. Meng⁴⁹, J. G. Messchendorp²⁹, G. Mezzadri^{24B}, J. Min^{1,43}, R. E. Mitchell²², X. H. Mo^{1,43,47}, Y. J. Mo⁶, C. Morales Morales¹⁵, N. Yu. Muchnoi^{10,d}, H. Muramatsu⁵⁰, A. Mustafa⁴, Y. Nefedov²⁷, F. Nerling¹¹, I. B. Nikolaev^{10,d}, Z. Ning^{1,43}, S. Nisar⁸, S. L. Niu^{1,43}, X. Y. Niu^{1,47}, S. L. Olsen^{36,k}, Q. Ouyang^{1,43,47}, S. Pacetti^{23B}, Y. Pan^{53,43}, M. Papenbrock⁵⁷, P. Patteri^{23A}, M. Pelizaeus⁴, J. Pellegrino^{56A,56C}, H. P. Peng^{53,43}, Z. Y. Peng¹³, K. Peters^{11,g}, J. Pettersson⁵⁷, J. L. Ping³², R. G. Ping^{1,47}, A. Pitka⁴, R. Poling⁵⁰, V. Prasad^{53,43}, H. R. Qi², M. Qi³³, T. Y. Qi², S. Qian^{1,43}, C. F. Qiao⁴⁷, N. Qin⁵⁸, X. S. Qin⁴, Z. H. Qin^{1,43}, J. F. Qiu¹, S. Q. Qu³⁴, K. H. Rashid^{55,i}, C. F. Redmer²⁶, M. Richter⁴, M. Ripka²⁶, A. Rivetti^{56C}, M. Rolo^{56C}, G. Rong^{1,47}, Ch. Rosner¹⁵, A. Sarantsev^{27,e}, M. Savrié^{24B}, K. Schoenning⁵⁷, W. Shan¹⁹, X. Y. Shan^{53,43}, M. Shao^{53,43}, C. P. Shen², P. X. Shen³⁴, X. Y. Shen^{1,47}, H. Y. Sheng¹, X. Shi^{1,43}, J. J. Song³⁷, W. M. Song³⁷, X. Y. Song¹, S. Sosio^{56A,56C}, C. Sowa⁴, S. Spataro^{56A,56C}, G. X. Sun¹, J. F. Sun¹⁶, L. Sun⁵⁸, S. S. Sun^{1,47}, X. H. Sun¹, Y. J. Sun^{53,43}, Y. K. Sun^{53,43}, Y. Z. Sun¹, Z. J. Sun^{1,43}, Z. T. Sun¹, Y. T. Tan^{53,43}, C. J. Tang⁴⁰, G. Y. Tang¹, X. Tang¹, I. Tapan^{46C}, M. Tiemens²⁹, B. Tsednee²⁵, I. Uman^{46D}, B. Wang¹, B. L. Wang⁴⁷, D. Wang³⁵, D. Y. Wang³⁵, Dan Wang⁴⁷, K. Wang^{1,43}, L. L. Wang¹, L. S. Wang¹, M. Wang³⁷, Meng Wang^{1,47}, P. Wang¹, P. L. Wang¹, W. P. Wang^{53,43}, X. F. Wang⁴⁵, X. L. Wang^{9,j}, Y. Wang^{53,43}, Y. F. Wang^{1,43,47}, Z. Wang^{1,43}, Z. G. Wang^{1,43}, Z. Y. Wang¹, Zongyuan Wang^{1,47}, T. Weber⁴, D. H. Wei¹², P. Weidenkaff²⁶, S. P. Wen¹, U. Wiedner⁴, M. Wolke⁵⁷, L. H. Wu¹, L. J. Wu^{1,47}, Z. Wu^{1,43}, L. Xia^{53,43}, Y. Xia²⁰, D. Xiao¹, Y. J. Xiao^{1,47}, Z. J. Xiao³², Y. G. Xie^{1,43}, Y. H. Xie⁶, X. A. Xiong^{1,47}, Q. L. Xiu^{1,43}, G. F. Xu¹, J. J. Xu^{1,47}, L. Xu¹, Q. J. Xu¹⁴, Q. N. Xu⁴⁷, X. P. Xu⁴¹, F. Yan⁵⁴, L. Yan^{56A,56C}, W. B. Yan^{53,43}, W. C. Yan², Y. H. Yan²⁰, H. J. Yang^{38,h}, H. X. Yang¹, L. Yang⁵⁸, R. X. Yang^{53,43}, Y. H. Yang³³, Y. X. Yang¹², Yifan Yang^{1,47}, Z. Q. Yang²⁰, M. Ye^{1,43}, M. H. Ye⁷, J. H. Yin¹, Z. Y. You⁴⁴, B. X. Yu^{1,43,47}, C. X. Yu³⁴, J. S. Yu²⁰, J. S. Yu³⁰, C. Z. Yuan^{1,47}, Y. Yuan¹, A. Yuncu^{46B,a}, A. A. Zafar⁵⁵, Y. Zeng²⁰, B. X. Zhang¹, B. Y. Zhang^{1,43}, C. C. Zhang¹, D. H. Zhang¹, H. H. Zhang⁴⁴, H. Y. Zhang^{1,43}, J. Zhang^{1,47}, J. L. Zhang⁵⁹, J. Q. Zhang⁴, J. W. Zhang^{1,43,47}, J. Y. Zhang¹, J. Z. Zhang^{1,47}, K. Zhang^{1,47}, L. Zhang⁴⁵, T. J. Zhang^{38,h}, X. Y. Zhang³⁷, Y. Zhang^{53,43}, Y. H. Zhang^{1,43}, Y. T. Zhang^{53,43}, Yang Zhang¹, Yao Zhang¹, Yi Zhang^{9,j}, Yu Zhang⁴⁷, Z. H. Zhang⁶, Z. P. Zhang⁵³, Z. Y. Zhang⁵⁸, G. Zhao¹, J. W. Zhao^{1,43}, J. Y. Zhao^{1,47}, J. Z. Zhao^{1,43}, Lei Zhao^{53,43}, Ling Zhao¹, M. G. Zhao³⁴, Q. Zhao¹, S. J. Zhao⁶¹, T. C. Zhao¹, Y. B. Zhao^{1,43}, Z. G. Zhao^{53,43}, A. Zhemchugov^{27,b}, B. Zheng⁵⁴, J. P. Zheng^{1,43}, Y. H. Zheng⁴⁷, B. Zhong³², L. Zhou^{1,43}, Q. Zhou^{1,47}, X. Zhou⁵⁸, X. K. Zhou^{53,43}, X. R. Zhou^{53,43}, X. Y. Zhou¹, Xiaoyu Zhou²⁰, Xu Zhou²⁰, A. N. Zhu^{1,47}, J. Zhu³⁴, J. Zhu⁴⁴, K. Zhu¹, K. J. Zhu^{1,43,47}, S. Zhu¹, S. H. Zhu⁵², X. L. Zhu⁴⁵, Y. C. Zhu^{53,43}, Y. S. Zhu^{1,47}, Z. A. Zhu^{1,47}, J. Zhuang^{1,43}, B. S. Zou¹, J. H. Zou¹

(BESIII Collaboration)

¹ Institute of High Energy Physics, Beijing 100049, People's Republic of China

² Beihang University, Beijing 100191, People's Republic of China

³ Beijing Institute of Petrochemical Technology, Beijing 102617, People's Republic of China

⁴ Bochum Ruhr-University, D-44780 Bochum, Germany

- ⁵ Carnegie Mellon University, Pittsburgh, Pennsylvania 15213, USA
- ⁶ Central China Normal University, Wuhan 430079, People's Republic of China
- ⁷ China Center of Advanced Science and Technology, Beijing 100190, People's Republic of China
- ⁸ COMSATS Institute of Information Technology, Lahore, Defence Road, Off Raiwind Road, 54000 Lahore, Pakistan
- ⁹ Fudan University, Shanghai 200443, People's Republic of China
- ¹⁰ G.I. Budker Institute of Nuclear Physics SB RAS (BINP), Novosibirsk 630090, Russia
- ¹¹ GSI Helmholtzcentre for Heavy Ion Research GmbH, D-64291 Darmstadt, Germany
- ¹² Guangxi Normal University, Guilin 541004, People's Republic of China
- ¹³ Guangxi University, Nanning 530004, People's Republic of China
- ¹⁴ Hangzhou Normal University, Hangzhou 310036, People's Republic of China
- ¹⁵ Helmholtz Institute Mainz, Johann-Joachim-Becher-Weg 45, D-55099 Mainz, Germany
- ¹⁶ Henan Normal University, Xinxiang 453007, People's Republic of China
- ¹⁷ Henan University of Science and Technology, Luoyang 471003, People's Republic of China
- ¹⁸ Huangshan College, Huangshan 245000, People's Republic of China
- ¹⁹ Hunan Normal University, Changsha 410081, People's Republic of China
- ²⁰ Hunan University, Changsha 410082, People's Republic of China
- ²¹ Indian Institute of Technology Madras, Chennai 600036, India
- ²² Indiana University, Bloomington, Indiana 47405, USA
- ²³ (A)INFN Laboratori Nazionali di Frascati, I-00044, Frascati, Italy; (B)INFN and University of Perugia, I-06100, Perugia, Italy
- ²⁴ (A)INFN Sezione di Ferrara, I-44122, Ferrara, Italy; (B)University of Ferrara, I-44122, Ferrara, Italy
- ²⁵ Institute of Physics and Technology, Peace Ave. 54B, Ulaanbaatar 13330, Mongolia
- ²⁶ Johannes Gutenberg University of Mainz, Johann-Joachim-Becher-Weg 45, D-55099 Mainz, Germany
- ²⁷ Joint Institute for Nuclear Research, 141980 Dubna, Moscow region, Russia
- ²⁸ Justus-Liebig-Universität Giessen, II. Physikalisches Institut, Heinrich-Buff-Ring 16, D-35392 Giessen, Germany
- ²⁹ KVI-CART, University of Groningen, NL-9747 AA Groningen, The Netherlands
- ³⁰ Lanzhou University, Lanzhou 730000, People's Republic of China
- ³¹ Liaoning University, Shenyang 110036, People's Republic of China
- ³² Nanjing Normal University, Nanjing 210023, People's Republic of China
- ³³ Nanjing University, Nanjing 210093, People's Republic of China
- ³⁴ Nankai University, Tianjin 300071, People's Republic of China
- ³⁵ Peking University, Beijing 100871, People's Republic of China
- ³⁶ Seoul National University, Seoul, 151-747 Korea
- ³⁷ Shandong University, Jinan 250100, People's Republic of China
- ³⁸ Shanghai Jiao Tong University, Shanghai 200240, People's Republic of China
- ³⁹ Shanxi University, Taiyuan 030006, People's Republic of China
- ⁴⁰ Sichuan University, Chengdu 610064, People's Republic of China
- ⁴¹ Soochow University, Suzhou 215006, People's Republic of China
- ⁴² Southeast University, Nanjing 211100, People's Republic of China
- ⁴³ State Key Laboratory of Particle Detection and Electronics, Beijing 100049, Hefei 230026, People's Republic of China
- ⁴⁴ Sun Yat-Sen University, Guangzhou 510275, People's Republic of China
- ⁴⁵ Tsinghua University, Beijing 100084, People's Republic of China
- ⁴⁶ (A)Ankara University, 06100 Tandogan, Ankara, Turkey; (B)Istanbul Bilgi University, 34060 Eyup, Istanbul, Turkey; (C)Uludag University, 16059 Bursa, Turkey; (D)Near East University, Nicosia, North Cyprus, Mersin 10, Turkey
- ⁴⁷ University of Chinese Academy of Sciences, Beijing 100049, People's Republic of China
- ⁴⁸ University of Hawaii, Honolulu, Hawaii 96822, USA
- ⁴⁹ University of Jinan, Jinan 250022, People's Republic of China
- ⁵⁰ University of Minnesota, Minneapolis, Minnesota 55455, USA
- ⁵¹ University of Muenster, Wilhelm-Klemm-Str. 9, 48149 Muenster, Germany
- ⁵² University of Science and Technology Liaoning, Anshan 114051, People's Republic of China
- ⁵³ University of Science and Technology of China, Hefei 230026, People's Republic of China
- ⁵⁴ University of South China, Hengyang 421001, People's Republic of China
- ⁵⁵ University of the Punjab, Lahore-54590, Pakistan
- ⁵⁶ (A)University of Turin, I-10125, Turin, Italy; (B)University of Eastern Piedmont, I-15121, Alessandria, Italy; (C)INFN, I-10125, Turin, Italy
- ⁵⁷ Uppsala University, Box 516, SE-75120 Uppsala, Sweden
- ⁵⁸ Wuhan University, Wuhan 430072, People's Republic of China
- ⁵⁹ Xinyang Normal University, Xinyang 464000, People's Republic of China
- ⁶⁰ Zhejiang University, Hangzhou 310027, People's Republic of China
- ⁶¹ Zhengzhou University, Zhengzhou 450001, People's Republic of China

^a Also at Bogazici University, 34342 Istanbul, Turkey

^b Also at the Moscow Institute of Physics and Technology, Moscow 141700, Russia

^c Also at the Functional Electronics Laboratory, Tomsk State University, Tomsk, 634050, Russia

^d Also at the Novosibirsk State University, Novosibirsk, 630090, Russia

^e Also at the NRC "Kurchatov Institute", PNPI, 188300, Gatchina, Russia

^f Also at Istanbul Arel University, 34295 Istanbul, Turkey

^g Also at Goethe University Frankfurt, 60323 Frankfurt am Main, Germany

^h Also at Key Laboratory for Particle Physics, Astrophysics and Cosmology, Ministry of Education; Shanghai Key Laboratory for Particle Physics and Cosmology; Institute of Nuclear and Particle Physics, Shanghai 200240, People's Republic of China

ⁱ Government College Women University, Sialkot - 51310. Punjab, Pakistan.

^j Key Laboratory of Nuclear Physics and Ion-beam Application (MOE) and Institute of Modern Physics, Fudan University, Shanghai 200443, People's Republic of China

^k Currently at: Center for Underground Physics, Institute for Basic Science, Daejeon 34126, Korea

(Dated: June 11, 2019)

Using a data sample with an integrated luminosity of 2.93 fb^{-1} taken at the center-of-mass energy of 3.773 GeV , we search for the Majorana neutrino (ν_m) in the lepton number violating decays $D \rightarrow K\pi e^+e^+$. No significant signal is observed, and the upper limits on the branching fraction at the 90% confidence level are set to be $\mathcal{B}(D^0 \rightarrow K^-\pi^-e^+e^+) < 2.8 \times 10^{-6}$, $\mathcal{B}(D^+ \rightarrow K_S^0\pi^-e^+e^+) < 3.3 \times 10^{-6}$ and $\mathcal{B}(D^+ \rightarrow K^-\pi^0e^+e^+) < 8.5 \times 10^{-6}$. The Majorana neutrino is searched for with different mass assumptions ranging from 0.25 to $1.0 \text{ GeV}/c^2$ in the decays $D^0 \rightarrow K^-e^+\nu_m$, $\nu_m \rightarrow \pi^-e^+$ and $D^+ \rightarrow K_S^0e^+\nu_m$, $\nu_m \rightarrow \pi^-e^+$, and the upper limits on the branching fraction at the 90% confidence level are at the level of $10^{-7} \sim 10^{-6}$, depending on the mass of the Majorana neutrino. The constraints on the mixing matrix element $|V_{e\nu_m}|^2$ are also evaluated.

PACS numbers: 11.30.Fs, 13.35.Hb

I. INTRODUCTION

In the Standard Model (SM), due to the absence of a right-handed neutrino component and the requirements of $SU(2)_L$ gauge invariance and renormalizability, neutrinos are postulated to be massless. However, the observations of neutrino oscillation [1–4] have shown that neutrinos have a tiny mass, which provides the first evidence for physics beyond the SM. Theoretically, the leading model to accommodate the neutrino masses is the so-called “see-saw” mechanism, which can be realized in several different schemes [5–8]. In the canonical case, the mass (m_ν) of an observed light neutrino is given by $m_\nu \sim y_\nu^2 v^2 / m_{\nu_m}$, where y_ν is a Yukawa coupling of a light neutrino to the Higgs field, v is the Higgs vacuum expectation value in the SM, and m_{ν_m} is the mass of a new massive neutrino state ν_m . The smallness of m_ν can be attributed to the existence of the new neutrino state ν_m with high mass.

The nature of neutrinos, whether neutrinos are Dirac or Majorana particles, is still an open question. If they are Majorana, their particles and antiparticles are identical, while they are not identical if they are Dirac particles. The effects of Majorana neutrino can be manifested through the processes violating lepton-number (L) conservation by two units ($\Delta L = 2$). Consequently, experimental searches for Majorana neutrinos occurring through lepton-number violating (LNV) $\Delta L = 2$ processes are of great interest. Different $\Delta L = 2$ processes at low and high energies have been proposed in the literatures [9–13]. Among them, an interesting source of LNV processes is given by exchanging a single Majorana neutrino with a mass on the order of the heavy flavor mass scale, where the Majorana neutrino can be kinematically accessible and produced on shell. The effects of such a

heavy neutrino with mass in the range $100 \text{ MeV}/c^2$ to a few GeV/c^2 have been widely searched for in $\Delta L = 2$ three-body and four-body decays of heavy flavor mesons and in τ lepton decays by different experiments, as summarized in Ref. [14], but no evidence has been observed so far. The $\Delta L = 2$ processes of D mesons have been reported by the E791 collaboration [15] with upper limits (ULs) on the decay branching fraction (BF) ranging $10^{-5} \sim 10^{-4}$.

In this paper, we present the studies of LNV processes with $\Delta L = 2$ in D meson decays $D^0 \rightarrow K^-\pi^-e^+e^+$, $D^+ \rightarrow K_S^0\pi^-e^+e^+$ and $D^+ \rightarrow K^-\pi^0e^+e^+$. These processes can occur through Cabibbo-favored (CF) and doubly Cabibbo-suppressed (DCS) decays by mediation of a Majorana neutrino, ν_m [11], as depicted in Fig. 1. The DCS processes (Figs. 1(c) and 1(d)) are expected to be suppressed by a factor $|V_{cd}V_{us}/V_{cs}V_{ud}| \sim 0.05$ [16] with respect to the CF processes (Figs. 1(a) and 1(b)). In this analysis, we search for the above three processes as well as the Majorana neutrino with different m_{ν_m} hypotheses in the CF processes. Additionally, the constraints on the mixing matrix element $|V_{e\nu_m}|^2$ are also estimated depending on m_{ν_m} . The analysis is carried out based on the data sample with an integrated luminosity of 2.93 fb^{-1} at the center-of-mass (C.M.) energy (\sqrt{s}) of 3.773 GeV collected with the BESIII detector. Throughout the paper, the charged conjugated modes are always implied implicitly.

II. DETECTOR AND MONTE CARLO SIMULATION

The BESIII detector is a magnetic spectrometer [17] located at the Beijing Electron Positron Collider

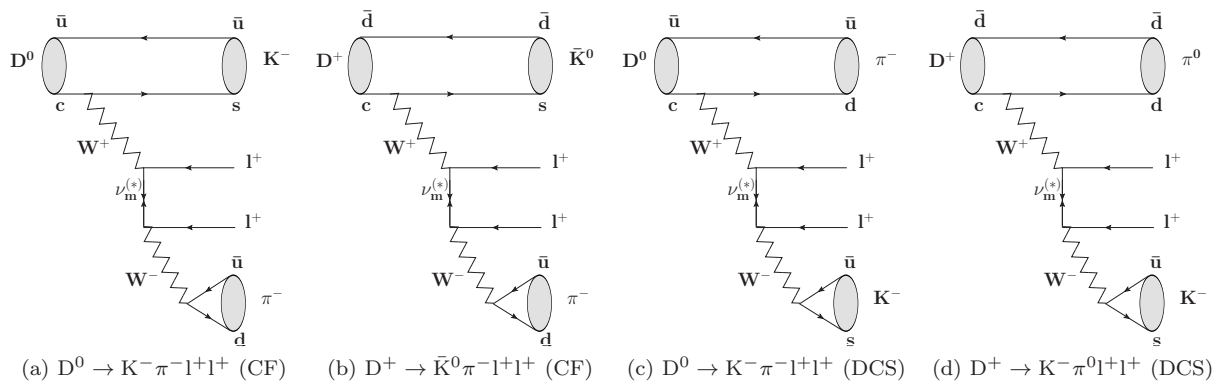


FIG. 1. Feynman diagrams for LNV processes $D \rightarrow K \pi l^+ l^+$ involving the Majorana neutrino ($\nu_m^{(*)}$), where l means the lepton.

(BEPCCII) [18]. The cylindrical core of the BESIII detector consists of a helium-based multilayer drift chamber (MDC), a plastic scintillator time-of-flight system (TOF), and a CsI(Tl) electromagnetic calorimeter (EMC), which are all enclosed in a superconducting solenoidal magnet providing a 1.0 T magnetic field. The solenoid is supported by an octagonal flux-return yoke with resistive plate counter muon identifier modules interleaved with steel. The acceptance of charged particles and photons is 93% over 4π solid angle. The charged-particle momentum resolution at 1 GeV/c is 0.5%, and the dE/dx resolution is 6% for the electrons from Bhabha scattering. The EMC measures photon energies with a resolution of 2.5% (5%) at 1 GeV in the barrel (end cap) region. The time resolution of the TOF is 68 ps (110 ps) in barrel (end-cap).

Simulated samples produced with the GEANT4-based [19] Monte Carlo (MC) program which includes the geometric description of the BESIII detector and the detector response, are used to determine the detection efficiency and to estimate the backgrounds. The simulation includes the beam energy spread and initial state radiation (ISR) in the e^+e^- annihilations modeled with the generator KKMC [20].

The cocktail MC sample consists of the production of $D\bar{D}$ pairs with consideration of quantum coherence for all neutral D decay modes, the non- $D\bar{D}$ decays of the $\psi(3770)$, the ISR production of the J/ψ and $\psi(3686)$ states, and the continuum processes incorporated in KKMC [20]. The known decay modes are modeled with EVTGEN [21] using BFs taken from the Particle Data Group [16], and the remaining unknown decays from the charmonium states with LUNDCHARM [22]. Final state radiation (FSR) from charged final state particles are incorporated with the PHOTOS package [23]. The cocktail MC sample is generated to study the possible background sources, and is normalized to the luminosity of the data sample in the analysis.

To study the detector efficiencies of the LNV $\Delta L = 2$ processes, the signal D meson is assumed to decay uniformly in phase space, while in searching for the

Majorana neutrino, the exclusive MC samples $D^0 \rightarrow K^- e^+ \nu_m$ and $D^+ \rightarrow K_S^0 e^+ \nu_m$ with $\nu_m \rightarrow \pi^- e^+$ are generated with different m_{ν_m} assumptions, and the angular distributions are simulated according to the squared amplitude in Eq. (8) of Ref. [11]. The form factor is described with the modified pole approximation.

III. EVENT SELECTION

Charged tracks in a candidate event are reconstructed from hits in the MDC. The charged tracks other than those from K_S^0 decay are required to pass within 10 cm of the interaction point (IP) in the beam direction and within 1 cm in the plane perpendicular to the beam, as well as satisfy $|\cos\theta| < 0.93$, where θ is the polar angle relative to the beam direction. The TOF and dE/dx information are combined to determine particle identification (PID) probabilities ($prob$) for the π and K hypotheses, and a π (K) is identified by requiring $prob(\pi) > prob(K)$ ($prob(K) > prob(\pi)$). To identify an electron or positron, the EMC information is also used to determine the PID probability. An electron or positron is required to satisfy $prob(e)/(prob(e) + prob(\pi) + prob(K)) > 0.8$, and $E/p > 0.8$, where E and p are the deposited energy in the EMC and the track momentum measured in the MDC, respectively.

The K_S^0 candidates are reconstructed with a vertex-constrained fit for pairs of oppositely charged tracks, assumed to be pions, which are required to pass within 20 cm of the IP along the beam direction, but with no constraint in the transverse plane. A vertex fit is carried out to insure that the two selected tracks originate from a common vertex, and the fit χ^2 is required to be less than 100. The resulting decay vertex is required to be separated from the IP by greater than twice the resolution. The K_S^0 candidates are further required to have an invariant mass within $[0.487, 0.511]$ GeV/ c^2 .

Electromagnetic showers are reconstructed from clusters of energy deposited in the EMC, and the energy deposited in nearby TOF counters is included to im-

prove the reconstruction efficiency and energy resolution. Photon candidate showers must have a minimum energy of 25 MeV in the barrel region ($|\cos\theta| < 0.80$) or 50 MeV in the end-cap region ($0.86 < |\cos\theta| < 0.92$). To suppress showers originating from charged particles, a photon must be separated by at least 10° from any charged track. To suppress electronic noise and energy deposits unrelated to the event, timing information from the EMC for the photon candidates must be in coincidence with collision events i.e., $0 \leq t \leq 700$ ns. The π^0 candidates are reconstructed from pairs of photons. Due to the worse resolution in the EMC end-caps, π^0 candidates reconstructed with two photons in the end-caps of the EMC are rejected. The invariant mass of two photons is required to be within $[0.115, 0.150]$ GeV/ c^2 for π^0 candidates. In the following analysis, the photon pair is kinematically constrained to the nominal mass of the π^0 to improve the resolution of π^0 momentum.

In order to improve the positron momentum resolution for the effects of FSR and bremsstrahlung, we use an FSR recovery process, where any photon, which has energy greater than 30 MeV, is separated by more than 20° from any shower in the EMC originating from a charged track, and is within a cone of 5° around the positron direction, has its momentum added to that of the positron.

In the analysis, the signal candidates of D meson LNV decay are searched for using a single tag (ST) method. Two variables, the beam energy constrained mass M_{BC} and the energy difference ΔE ,

$$\begin{aligned} M_{BC} &= \sqrt{E_{\text{beam}}^2 - |\vec{p}_D|^2}, \\ \Delta E &= E_D - E_{\text{beam}}, \end{aligned} \quad (1)$$

are used to identify the signal candidates, where \vec{p}_D and E_D are the momentum and energy of the D candidates in the e^+e^- C.M. system, and E_{beam} is the beam energy. The D meson decays form a peak at the nominal D mass in the M_{BC} distribution and at zero in the ΔE spectra. If multiple candidates are present per charm per event, the one with the smallest $|\Delta E|$ is chosen. Candidate events with M_{BC} greater than 1.84 GeV/ c^2 and ΔE within approximately $[-3.5, 2.5]$ standard deviations of the peak are accepted. The numerical values of the mode dependent ΔE requirement are listed in Table I.

TABLE I. ΔE requirements for $D \rightarrow K\pi e^+e^+$ processes.

Channel	ΔE (MeV)
$D^0 \rightarrow K^- \pi^- e^+ e^+$	$[-33.0, 19.7]$
$D^+ \rightarrow K_S^0 \pi^- e^+ e^+$	$[-30.6, 19.3]$
$D^+ \rightarrow K^- \pi^0 e^+ e^+$	$[-54.8, 24.4]$

Potential background sources are examined with the cocktail MC sample. The dominant contributions are from the processes $\psi(3770) \rightarrow D\bar{D}$ with $D \rightarrow K e \nu_e$ due

to large BFs and the processes $e^+e^- \rightarrow q\bar{q}$, but no peaking background is observed in the M_{BC} distribution.

IV. SIGNAL DETERMINATION

The signal yields are determined by performing an unbinned maximum likelihood fit on the M_{BC} distribution of surviving candidate events. In the fit, the background shape is described by an ARGUS function [24], and the signal shape is modeled by the MC simulated shape convolved with a Gaussian function which accounts for the resolution difference between data and MC simulation. The width of the Gaussian function is fixed to be 0.32 MeV/ c^2 , obtained from a control sample of $D^0 \rightarrow K^- \pi^+ \pi^+ \pi^-$ decay. The fits are shown in Fig. 2. The BFs, $\mathcal{B}_{D \rightarrow K\pi e^+e^+}$, are calculated by

$$\mathcal{B}_{D \rightarrow K\pi e^+e^+} = \frac{N_{\text{sig}}}{2 \cdot N_{D\bar{D}}^{\text{tot}} \cdot \epsilon \cdot \mathcal{B}}, \quad (2)$$

where N_{sig} is the signal yield determined from the fit, $N_{D\bar{D}}^{\text{tot}}$ is the total number of $D\bar{D}$ pairs, which are $(8, 296 \pm 31 \pm 65) \times 10^3$ for D^+D^- pairs and $(10, 597 \pm 28 \pm 98) \times 10^3$ for $D^0\bar{D}^0$ pairs [25], ϵ is the detection efficiency, obtained from the corresponding MC simulation, and \mathcal{B} is the decay branching fraction of the intermediate state, i.e., 1 in the decay $D^0 \rightarrow K^- \pi^- e^+ e^+$ due to no intermediate state involved, $\mathcal{B}_{K_S^0 \rightarrow \pi^+ \pi^-}$ in the decay $D^+ \rightarrow K_S^0 \pi^- e^+ e^+$ and $\mathcal{B}_{\pi^0 \rightarrow \gamma\gamma}$ in the decay $D^+ \rightarrow K^- \pi^0 e^+ e^+$, where $\mathcal{B}_{K_S^0 \rightarrow \pi^+ \pi^-}$ and $\mathcal{B}_{\pi^0 \rightarrow \gamma\gamma}$ are taken from the world average values [16]. A factor of 2 in the denominator indicates both D and \bar{D} mesons in every event are included.

Since no obvious signal is observed, the ULs at the 90% confidence level (CL) on the BFs of $D \rightarrow K\pi e^+e^+$ decays are set after considering the effect of systematic uncertainties.

V. SYSTEMATIC UNCERTAINTIES

The systematic uncertainties arise from several aspects including the tracking and PID efficiencies of charged tracks, K_S^0 and π^0 reconstruction efficiencies, total number of $D\bar{D}$ pairs, BFs of $K_S^0 \rightarrow \pi^+ \pi^-$ and $\pi^0 \rightarrow \gamma\gamma$ decays, ΔE requirement, FSR recovery, modeling for detection efficiency and fitting M_{BC} .

Systematic uncertainties from the tracking efficiency of K , π and e are assigned to be 1.0% per track [26, 27]. For the PID efficiency, the systematic uncertainties for $K(\pi)$ and e are 0.5% and 1.0% per track [26, 27], respectively. Systematic uncertainties from K_S^0 and π^0 reconstruction are taken to be 1.5% and 2% [28], respectively.

The systematic uncertainty of the total number of $D\bar{D}$ pairs is 0.9% [25]. The BFs of $K_S^0 \rightarrow \pi^+ \pi^-$ and $\pi^0 \rightarrow \gamma\gamma$ are $(69.20 \pm 0.05)\%$ and $(98.823 \pm 0.034)\%$ from the world average values [16], resulting in the systematic uncertainty of 0.1% and 0.0%, respectively.

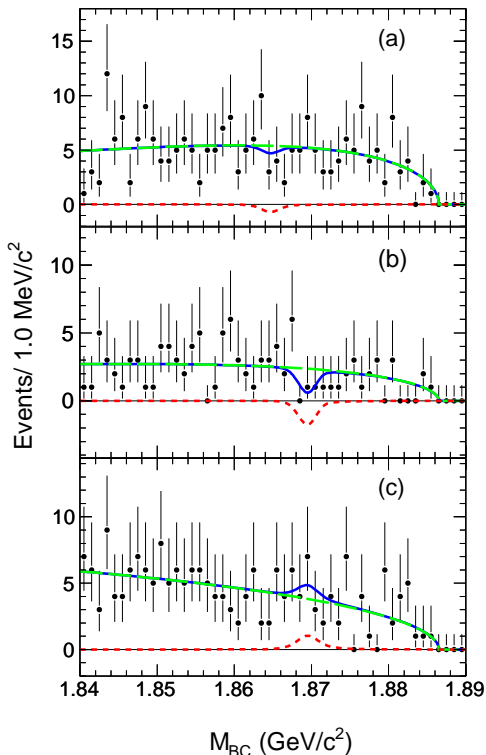


FIG. 2. (color online) Fitting on the M_{BC} spectra for the decays (a) $D^0 \rightarrow K^- \pi^- e^+ e^+$, (b) $D^+ \rightarrow K_S^0 \pi^- e^+ e^+$ and (c) $D^+ \rightarrow K^- \pi^0 e^+ e^+$. The dotted points with error bars are from data, the blue lines are the fitting result, the dashed red and long dashed green lines are the signal and background components, respectively.

The systematic uncertainty from the ΔE requirement is studied using control samples of $D^0 \rightarrow K^- \pi^+ \pi^0$ and $D^+ \rightarrow K^+ \pi^+ \pi^-$ for the signal processes with and without π^0 in final states, where the control samples are selected with the ST method. We set $[\mu - 3.5\sigma, \mu + 2.5\sigma]$ as a nominal ΔE window for the signal, where μ and σ are the mean and width values of ΔE obtained by fitting. Then we vary the ΔE window by 0.5σ on both sides, and the resulting differences of the change of efficiency between data and MC simulation are taken as the systematic uncertainties.

To study the systematic uncertainty associated with FSR recovery process, we obtain the alternative detection efficiency without the FSR recovery process, and the difference in the efficiency is taken as the systematic uncertainty.

The difference of the geometric efficiency between the one obtained with the phase space generator, and the average of m_{ν_m} -dependent cases, is taken as the systematic uncertainty associated with the modeling.

The systematic uncertainty associated with the fitting of the M_{BC} distribution arises from the fitting range, sig-

nal shape and background shape. We performed alternative fits by varying the fitting range from $[1.84, 1.89]$ to $[1.845, 1.89]$ GeV/c^2 , the width of convolved Gaussian for signal shape within one standard deviation, and the background shape from the ARGUS function to the cocktail MC simulated shape. The relative changes of the signal yields are taken as the corresponding systematic uncertainties, and are found to be negligible compared to the statistical uncertainties.

All the systematic uncertainties are summarized in Table II. Assuming they are independent, the total systematic uncertainty is the quadrature sum of the individual ones.

VI. RESULTS AND DISCUSSION

A. Upper limits for $D \rightarrow K \pi e^+ e^+$ decays

Taking into account the effect of systematic uncertainties, we calculate ULs on the BFs for the LNV $\Delta L = 2$ decays $D^0 \rightarrow K^- \pi^- e^+ e^+$, $D^+ \rightarrow K_S^0 \pi^- e^+ e^+$ and $D^+ \rightarrow K^- \pi^0 e^+ e^+$ according to Eq. (2) based on the Bayesian method [29]. A series of fits of the M_{BC} distribution are carried out fixing the BF at different values, and the resultant curve of likelihood values as a function of the BF is convolved with a Gaussian function, which has a width given by the overall systematic uncertainty and is normalized to the maximum value of 1. The ULs on the BF at the 90% CL, $\mathcal{B}_{\text{sig}}^{\text{UL}}$ for the different processes, which are listed in Table III, are the values that yield 90% of the likelihood integral over BF from zero to infinity.

B. Searching for Majorana neutrino

With the above three decay processes, the Majorana neutrino can be searched for by studying the decay chains $D^0 \rightarrow K^- e^+ \nu_m (\pi^- e^+)$, $D^+ \rightarrow K_S^0 e^+ \nu_m (\pi^- e^+)$ or $D^+ \rightarrow \pi^0 e^+ \nu_m (K^- e^+)$; a narrow peak will be present in the distribution of $\pi^- e^+$ ($K^- e^+$) invariant mass if a signal exists. Compared to the other two decay channels, the $D^+ \rightarrow \pi^0 e^+ \nu_m (K^- e^+)$ is expected to be suppressed by a factor of 1/20 because of the smaller CKM factors. So in this analysis, the Majorana neutrino is searched in the processes $D^0 \rightarrow K^- e^+ \nu_m (\pi^- e^+)$ and $D^+ \rightarrow K_S^0 e^+ \nu_m (\pi^- e^+)$ with different m_{ν_m} hypotheses, i.e., from 0.25 to 1.0 GeV/c^2 with an interval of 0.05 GeV/c^2 .

Based on the above selection criteria, to search for the Majorana neutrino with a given mass, m_{ν_m} , the candidate events are selected by further requiring the invariant mass of any $\pi^- e^+$ combination (two e^+ per event), $M_{\pi^- e^+}$, to be within the range of $[m_{\nu_m} - 3\sigma, m_{\nu_m} + 3\sigma]$, where σ is the resolution of the $M_{\pi^- e^+}$ distribution obtained by studying the signal MC sample. The number counting method is used to determine the signal yields

TABLE II. Relative systematic uncertainties for the $D \rightarrow K\pi e^+e^+$ processes (in percent). Here ‘-’ denotes that there is no corresponding systematic uncertainty, and ‘...’ means that the corresponding systematic uncertainty is negligible.

Source	Relative systematic uncertainty (%)		
	$D^0 \rightarrow K^-\pi^-e^+e^+$	$D^+ \rightarrow K_S^0\pi^-e^+e^+$	$D^+ \rightarrow K^-\pi^0e^+e^+$
Tracking	4.0	3.0	3.0
PID	3.0	2.5	2.5
K_S^0 selection	-	1.5	-
π^0 selection	-	-	2.0
$N_{D\bar{D}}$	1.0	0.9	0.9
Cited BF	-	0.1	0.0
ΔE requirement	0.7	0.7	0.4
FSR recovery	0.6	0.8	0.6
Efficiency modeling	3.6	4.3	4.7
Fitting M_{BC}
Total	6.3	6.2	6.5

TABLE III. The detection efficiencies (ϵ), the ULs at the 90% CL on the signal yields ($N_{\text{sig}}^{\text{UL}}$), and the BFs ($\mathcal{B}_{\text{sig}}^{\text{UL}}$) of $D \rightarrow K\pi e^+e^+$ processes.

Channel	$\epsilon(\%)$	$N_{\text{sig}}^{\text{UL}}$	$\mathcal{B}_{\text{sig}}^{\text{UL}}(\times 10^{-6})$
$D^0 \rightarrow K^-\pi^-e^+e^+$	16.8	10.0	< 2.8
$D^+ \rightarrow K_S^0\pi^-e^+e^+$	11.5	4.4	< 3.3
$D^+ \rightarrow K^-\pi^0e^+e^+$	10.6	14.8	< 8.5

due to very few events surviving. We count the number of signal candidates within the M_{BC} signal region of [1.859, 1.872] ([1.865, 1.875]) GeV/c^2 for the decay $D^0 \rightarrow K^-e^+\nu_m(\pi^-e^+)$ ($D^+ \rightarrow K_S^0e^+\nu_m(\pi^-e^+)$). The number of background events is estimated from the side-band regions of the M_{BC} distribution, defined as [1.842, 1.852] and [1.876, 1.886] ([1.842, 1.854] and [1.878, 1.886]) GeV/c^2 , taking into account the scale factor obtained by fitting the M_{BC} distribution as shown in Fig. 2. The ULs on the BF of Majorana neutrino case are calculated with the profile likelihood method incorporating the systematic uncertainty with TROLKE [30, 31] in the ROOT framework, where the numbers of events in the signal and side-band regions are assumed to be described by Poisson distributions and the efficiency by a Gaussian distribution. The ULs on the BF at the 90% CL as a function of m_{ν_m} are at the level of $10^{-7} \sim 10^{-6}$, as shown in Fig. 3.

Based on the measured BF, the mixing matrix element $|V_{e\nu_m}|^2$ of a positron with the heavy Majorana neutrino in the charged current interaction [9, 14] as a function of m_{ν_m} can be obtained by Eq. (3) [11],

$$\frac{\Gamma(m_{\nu_m}, V_{e\nu_m}(m_{\nu_m}))}{\Gamma(m_{\nu_m}, V'_{e\nu_m}(m_{\nu_m}))} = \frac{|V_{e\nu_m}(m_{\nu_m})|^4}{|V'_{e\nu_m}(m_{\nu_m})|^4}, \quad (3)$$

where the decay width $\Gamma(m_{\nu_m}, V_{e\nu_m}(m_{\nu_m}))$ is proportional to its BF, and $\Gamma(m_{\nu_m}, V'_{e\nu_m}(m_{\nu_m}))$ is related to the BF given in Tables 4 and 5 of Ref. [11], based on the assumptions that the Majorana neutrino is on-shell and its width is negligible compared to the neutrino mass. The mixing matrix element $|V'_{e\nu_m}(m_{\nu_m})|^2$ is derived from a reanalysis of neutrinoless double beta decay experimental data [32]. The resultant ULs on the mixing matrix element $|V_{e\nu_m}|^2$ as a function of m_{ν_m} , which are also depicted in Fig. 3, provide complementary information in D meson decays.

VII. SUMMARY

Using the data sample with the integrated luminosity of 2.93 fb^{-1} collected at the C.M. energy $\sqrt{s} = 3.773 \text{ GeV}$, we perform a search for LNV $\Delta L = 2$ decays of $D \rightarrow K\pi e^+e^+$ as well as search for a Majorana neutrino with different mass hypotheses. No evidence of a signal is found. Therefore, using the Bayesian approach, we place 90% CL ULs on the decay BF for $D^0 \rightarrow K^-\pi^-e^+e^+$, $D^+ \rightarrow K_S^0\pi^-e^+e^+$ and $D^+ \rightarrow K^-\pi^0e^+e^+$ to be 2.8×10^{-6} , 3.3×10^{-6} and 8.5×10^{-6} , respectively. We also determine ULs, which are of the level $10^{-7} \sim 10^{-6}$, on the BF at the 90% CL for the decays $D^0 \rightarrow K^-e^+\nu_m(\pi^-e^+)$ and $D^+ \rightarrow K_S^0e^+\nu_m(\pi^-e^+)$ with different m_{ν_m} hypotheses within the range 0.25 to 1.0 GeV/c^2 . The constraints on the mixing element $|V_{e\nu_m}|^2$ depending on m_{ν_m} are also evaluated based on the related variables from Ref. [11] and the measured BF. The results provide the supplementary information in the study

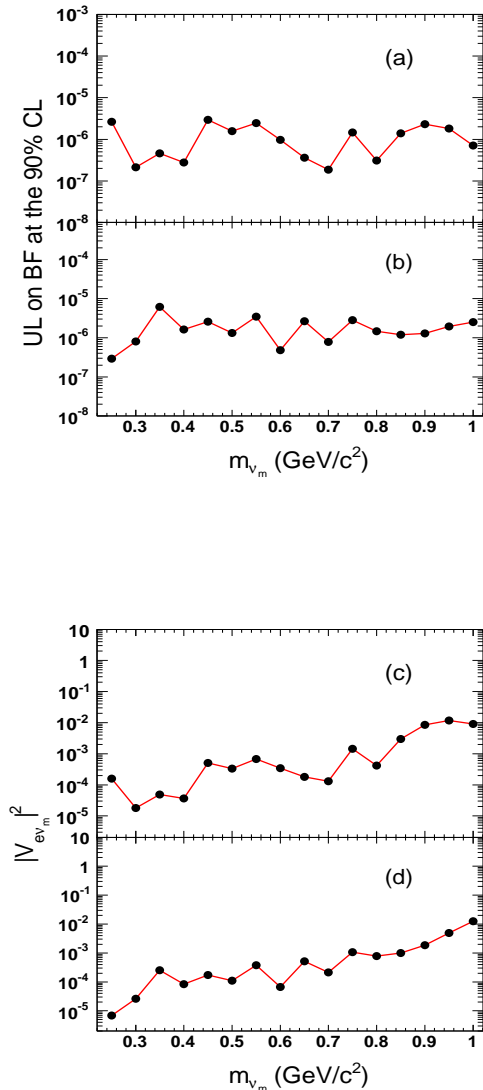


FIG. 3. The ULs on the (a)(b) BF and the (c)(d) mixing matrix element $|V_{e\nu_m}|^2$ at the 90% CL as a function of m_{ν_m} for the decays (a)(c) $D^0 \rightarrow K^- e^+ \nu_m (\pi^- e^+)$ and (b)(d) $D^+ \rightarrow K_S^0 e^+ \nu_m (\pi^- e^+)$.

of mixing between the heavy Majorana neutrino and the standard model neutrino ν_e in D meson decays.

ACKNOWLEDGEMENTS

The BESIII collaboration thanks the staff of BEPCII and the IHEP computing center for their strong support. This work is supported in part by National Key Basic Research Program of China under Contract No. 2015CB856700; National Natural Science Foundation of China (NSFC) under Contracts Nos. 11805037, 11235011, 11335008, 11425524, 11625523, 11635010; the Chinese Academy of Sciences (CAS) Large-Scale Scientific Facility Program; the CAS Center for Excellence in Particle Physics (CCEPP); Joint Large-Scale Scientific Facility Funds of the NSFC and CAS under Contracts Nos. U1832121, U1332201, U1532257, U1532258; CAS Key Research Program of Frontier Sciences under Contracts Nos. QYZDJ-SSW-SLH003, QYZDJ-SSW-SLH040; 100 Talents Program of CAS; National 1000 Talents Program of China; INPAC and Shanghai Key Laboratory for Particle Physics and Cosmology; German Research Foundation DFG under Contracts Nos. Collaborative Research Center CRC 1044, FOR 2359; Istituto Nazionale di Fisica Nucleare, Italy; Koninklijke Nederlandse Akademie van Wetenschappen (KNAW) under Contract No. 530-4CDP03; Ministry of Development of Turkey under Contract No. DPT2006K-120470; National Natural Science Foundation of China (NSFC) under Contracts Nos. 11505034, 11575077; National Science and Technology fund; The Swedish Research Council; U. S. Department of Energy under Contracts Nos. DE-FG02-05ER41374, DE-SC-0010118, DE-SC-0012069; University of Groningen (RuG) and the Helmholtzzentrum fuer Schwerionenforschung GmbH (GSI), Darmstadt; WCU Program of National Research Foundation of Korea under Contract No. R32-2008-000-10155-0.

[1] Y. Fukuda *et al.* (Super-Kamiokande Collaboration), Phys. Rev. Lett. **81**, 1562 (1998).
 [2] Q. R. Ahmad *et al.* (SNO Collaboration), Phys. Rev. Lett. **89**, 011301 (2002).
 [3] K. Eguchi *et al.* (KsmLAND Collaboration), Phys. Rev. Lett. **90**, 021802 (2003).
 [4] F. P. An *et al.* (DAYA-BAY Collaboration), Phys. Rev. Lett. **108**, 171803 (2012).

[5] H. Fritzsch, M. Gell-Mann and P. Minkowski, Phys. Lett. B **59**, 256 (1975); R. N. Mohapatra and G. Senjanović, Phys. Rev. Lett. **44**, 912 (1980).
 [6] W. Konetschny and W. Kummer, Phys. Lett. B **70**, 433 (1977); T. P. Cheng and L.-F. Li, Phys. Rev. D **22**, 2860 (1980); R. N. Mohapatra and G. Senjanović, Phys. Rev. D **23**, 165 (1981).
 [7] E. Ma, Phys. Rev. Lett. **81**, 1171 (1998); P. Fileviez Pérez, JHEP **03**, 142 (2009).

- [8] Z. Z. Xing and S. Zhou, High Energy Phys. Nucl. Phys. **30**, 828 (2006).
- [9] A. Atre, T. Han, S. Pascoli and B. Zhang, JHEP. **05**, 030 (2009).
- [10] G. López Castro and N. Quintero, Phys. Rev. D **87**, 07901 (2013).
- [11] H. R. Dong, F. Feng and H. B. Li, Chin. Phys. C **39**, 013101 (2015).
- [12] H. B. Li, Front. Phys. **12**, 121301 (2017).
- [13] D. Milanés and N. Quintero, Phys. Rev. D **98**, 096004 (2018).
- [14] D. Milanés, N. Quintero and C. E. Vera, Phys. Rev. D **93**, 094026 (2016).
- [15] E. Aitala *et al.* (E791 Collaboration), Phys. Rev. Lett **86**, 3969 (2001).
- [16] M. Tanabashi *et al.* (Particle Data Group), Phys. Rev. D **98**, 030001 (2018).
- [17] M. Ablikim *et al.* (BESIII Collaboration), Nucl. Instrum. Meth. A **614**, 345 (2010).
- [18] C. H. Yu *et al.*, Proceedings of IPAC2016, Busan, Korea, 2016, doi:10.18429/JACoW-IPAC2016-TUYA01.
- [19] S. Agostinelli *et al.* (GEANT4 Collaboration), Nucl. Instrum. Meth. A **506**, 250 (2003).
- [20] S. Jadach, B. F. L. Ward and Z. Was, Phys. Rev. D **63**, 113009 (2001); Comput. Phys. Commun. **130**, 260 (2000).
- [21] D. J. Lange, Nucl. Instrum. Meth. A **462**, 152 (2001); R. G. Ping, Chin. Phys. C **32**, 599 (2008).
- [22] J. C. Chen, G. S. Huang, X. R. Qi, D. H. Zhang and Y. S. Zhu, Phys. Rev. D **62**, 034003 (2000); R. L. Yang, R. G. Ping and H. Chen, Chin. Phys. Lett. **31**, 061301 (2014).
- [23] E. Richter-Was, Phys. Lett. B **303**, 163 (1993).
- [24] H. Albrecht *et al.* (ARGUS Collaboration), Phys. Lett. B **241**, 278 (1990).
- [25] M. Ablikim *et al.* (BESIII Collaboration), Chin. Phys. C **42**, 083001 (2018).
- [26] M. Ablikim *et al.* (BESIII Collaboration), Phys. Rev. Lett. **116**, 082001 (2016).
- [27] M. Ablikim *et al.* (BESIII Collaboration), Phys. Rev. D **92**, 072012 (2015).
- [28] M. Ablikim *et al.* (BESIII Collaboration), Eur. Phys. J. C **76**, 369 (2016).
- [29] Y. S. Zhu, Nucl. Instrum. Meth. A **578**, 289 (2007).
- [30] J. Conrad and J. Lundberg, Class in ROOT (2009).
- [31] W. A. Rolke, Angel M. Lópezb and J. Conrad, Nucl. Instrum. Meth. A **551**, 493 (2005).
- [32] P. Benes, A. Faessler, F. Simkovic and S. Kovalenko, Phys. Rev. D **71**, 077901 (2005).